Acta Math. Univ. Comenianae
Vol. LXXXIV, 2 (2015), pp. 243–253

HIGH ORDER COMBINATION TECHNIQUE FOR THE EFFICIENT PRICING OF BASKET OPTIONS

C. HENDRICKS, M. EHRHARDT AND M. GÜNTHER

Abstract. In computational finance, high dimensional problems typically arise when pricing basket options, foreign-exchange (FX) options, etc. Since the number of grid points grows exponentially with the dimension, the so called curse of dimensionality shows its effect very quickly. Sparse grids and the combination technique have proven their great ability to reduce the computational effort. In this article, we introduce a fourth order scheme for the combination technique to solve efficiently high dimensional partial differential equation problems. In order to linearly combine the sub-solutions, we propose a tensor-based interpolation method. We show that our approach can preserve the error splitting structure of the sub-solutions and lead to a highly accurate sparse grid solution.

1. Introduction

We consider the multi-dimensional Black-Scholes partial differential equation (PDE)

$$\frac{\partial u}{\partial t} + Lu = \frac{\partial u}{\partial t} + \frac{1}{2}\sum_{i,j=1}^{d} \rho_{ij}\sigma_i\sigma_j S_i S_j \frac{\partial^2 u}{\partial S_i \partial S_j} + \sum_{i=1}^{d}(r-q_i)S_i\frac{\partial u}{\partial S_i} - ru = 0. \tag{1}$$

The numerical approximation shall be computed on the space-time rectangle $\Omega_d \times \Omega_t$ with $\Omega_d = [0, S_1^{\max}] \times \cdots \times [0, S_d^{\max}]$, $\Omega_t = [0,T]$. The vector $\mathbf{S} := (S_1, \ldots, S_d)$ contains the single assets with volatility σ_i and correlation $\rho_{i,j}$ between assets S_i and S_j for $i,j = 1,\ldots,d$. The dividend paid on asset i is denoted by q_i. The terminal condition is given by the option's payoff $g(\mathbf{S})$, e.g.,

$$g(\mathbf{S}) := \Big(\sum_{i=1}^{d} w_k S_k - K\Big)^+, \qquad g(\mathbf{S}) := \Big(K - \sum_{i=1}^{d} w_k S_k\Big)^+$$

in the case of an European basket, call or put option with weights w_i for $i = 1,\ldots,d$ and strike price K. The constant r denotes the risk-free interest rate.

In order to solve the PDE numerically, usually a tensor based grid is employed. Since the number of involved grid points grows exponentially with the dimension d, we quickly reach a point where the computational effort makes it practically impossible to receive a solution in reasonable time with standard techniques. Hence it seems to be natural to ask for schemes which only need less grid points to

Received November 2, 2014; revised March 2, 2015.
2010 *Mathematics Subject Classification.* Primary 65M06, 65D05, 35Kxx.

achieve the desired accuracy. In this article, we want to tackle this problem in two ways. First, we introduce a finite difference scheme which is fourth order in space. Secondly, we apply the so called combination technique. This technique is based on linear combinination of a sequence of solutions via interpolation. In [**2, 8**], it is shown that compared to a full tensor based grid with mesh width h and $\mathcal{O}(h^{-d})$ grid points, the number of nodes can be reduced to $\mathcal{O}(h^{-1}\log(h^{-1})^{d-1})$, but keeping a high accuracy by cancellation of low order error terms. Furthermore, each sub-solution can be computed independently of the others and is therefore embarrassingly parallel.

2. Coordinate transformation and smoothing of initial data

With the help of a coordinate transformation, we can transform the PDE (1) into a form, that is advantageous from a numerical perspective. In the following, we discuss a coordinate transformation which aligns the payoff in one coordinate direction. Since it is well-known that the non-differentiability at the option's strike price has a negative impact on the order of convergence, we smooth the initial data [**4**] to recover a high rate of convergence. The alignment of the discontinuity allows us to apply the smoothing operator in just one coordinate direction, which reduces the computational effort.

2.1. Coordinate transformation

In the Black-Scholes PDE (1), the discontinuity of the payoff crosses all spatial dimensions. This makes it rather complicated to smooth the initial data or to use grid stretching methods to achieve a high order of convergence. Hence we use a non-linear transformation [**5, 6**] to align the payoff to one coordinate direction. The first coordinate direction is considered as the basket value and the other spatial dimensions are normalised to the $d-1$ dimensional unit cube. The transformation is given by

$$x_1 := \sum_{i=1}^{d} w_i S_i, \quad x_j := \frac{w_{j-1}S_{j-1}}{\sum_{i=j-1}^{d} w_i S_i} \text{ for } j \neq 1.$$

The payoff transforms to $g(x_1) = (x_1 - K)^+$, $g(x_1) = (K - x_1)^+$, respectively. Figure 1 shows the alignment of the discontinuity to the first coordinate direction.

The PDE (1) transforms to

$$\frac{\partial u}{\partial t} + Lu = \frac{\partial u}{\partial t} + \sum_{i,j=1}^{d} \alpha_{ij}\frac{\partial^2 u}{\partial x_i \partial x_j} + \sum_{i=1}^{d} \beta_i \frac{\partial u}{\partial x_i} - ru = 0 \tag{2}$$

in $\Omega_d \times \Omega_t$ with $\Omega_d = [0, x_1^{max}] \times [0,1]^{d-1}$, $\Omega_t = [0,T]$.

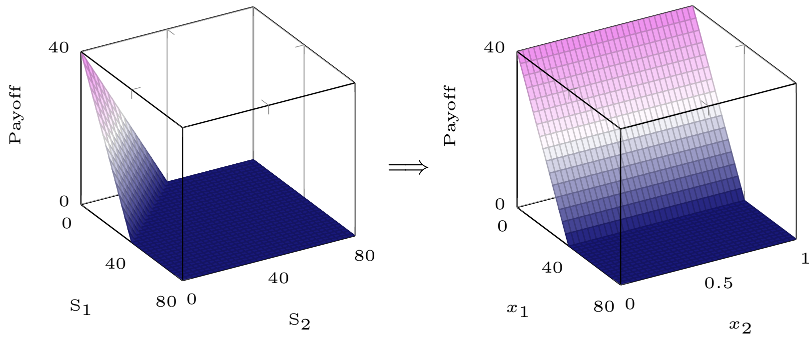

Figure 1. European 2-d basket put payoff without and with transformation.

The coefficient functions are given by

$$\alpha_{11} = x_1^2 \sum_{k,l=1}^{d} \hat{\rho}_{kl} f_{1,k} f_{1,l},$$

$$\alpha_{1j} = x_1 x_j (1 - x_j) \sum_{k,l=1}^{d} (\hat{\rho}_{k,l-1} - \hat{\rho}_{kl}) f_{1k} f_{1l},$$

$$\alpha_{ij} = x_i(1 - x_i) x_j (1 - x_j) \sum_{k,l=1}^{d} (\hat{\rho}_{kl} - \hat{\rho}_{i-1,l} - \hat{\rho}_{k,j-1} + \hat{\rho}_{i-1,j-1}) f_{ik} f_{jl}$$

and

$$\beta_1 := x_1 \sum_{k=1}^{d} (r - q_k) f_{1k},$$

$$\begin{aligned}\beta_i := x_i(1 - x_i) \sum_{k,l=1}^{d} \big(&- 2\hat{\rho}_{i-1,i-1} x_i + (2x_i - 1)(\hat{\rho}_{k,i-1} + \hat{\rho}_{l,i-1}) \\ &+ 2(1 - x_i)\hat{\rho}_{k,l} \big) f_{ik} f_{il} \\ + x_i(1 - x_i)\Big(r - q_1 - &\sum_{k=1}^{d} \big((r - q_k) f_{ik}\big) \Big)\end{aligned}$$

with

$$f_{il} := \begin{cases} x_{l+1} \prod_{j=i+1}^{l} (1 - x_j) & i < l < d \\ \prod_{j=i+1}^{l} (1 - x_j) & i < l = d \\ x_{l+1} & i = l < d \\ 1 & i = l = d \\ 0 & i > l \end{cases}$$

and $\hat{\rho}_{ij} = \frac{1}{2} \rho_{ij} \sigma_i \sigma_j$ for $i, j = 1, \ldots, d$. We see that (2) possesses the same structure as the original PDE (1), but different coefficient functions. Since it holds $\alpha_{ij} = 0$,

$\beta_j = 0$ for $x_j = \{0, 1\}$ with $i \geq 1$ and $j > 1$ and $\alpha_{i,1} = 0$, $\beta_i = 0$ for $x_1 = 0$, we do not need to prescribe any boundary conditions in these cases. Only at the upper limit of the truncated domain in the first coordinate direction, $x_1 = x_1^{\max}$, a boundary condition has to be specified. In the case of a put option the option's value can be set to zero and for call options the second derivative, can be considered as zero.

2.2. Smoothing of initial data

The consistency analysis of finite difference schemes (FDS) is in general based on Taylor expansion and draws from the assumption that the solution fulfills certain smoothness conditions. In practice the non-smoothness of the payoff leads to a reduced order of convergence. Kreiss et al. derived in their seminal paper [**4**] smoothing operators to recover the theoretical order of convergence. In the case of a fourth order scheme, we choose the following function $\hat{\Phi}_4$ in Fourier space

$$\hat{\Phi}_4(\omega) = \frac{\sin^4(\frac{1}{2}\omega) + \frac{2}{3}\sin^6(\frac{1}{2}\omega)}{(\frac{1}{2}\omega)^4}.$$

Then the smoothed initial values for the transformed problem (2) read

$$M_h g(x_0) = h^{-1} \int_{-3h}^{3h} \Phi_4(h^{-1}x) g(x_0 - x) \mathrm{d}x,$$

where Φ_4 denotes the Fourier inverse of $\hat{\Phi}_4$. Please note that Φ_4 is piecewise a polynomial of degree three and hence the integral can be solved analytically.

3. Finite difference scheme

The PDE (2) is solved via a FDS. In order to discretise the first, second and mixed derivatives in space, we apply the following fourth order finite difference stencils and assume the solution to be sufficiently smooth

$$\begin{aligned}
D_{x_i} u &= \frac{1}{12h_i}(-u_{k+2} + 8u_{k+1} - 8u_{k-1} + u_{k-2}) = \frac{\partial u}{\partial x_i} + \mathcal{O}(h_i^4), \\
D_{x_i}^2 u &= \frac{1}{12h_i^2}(-u_{k+2} + 16u_{k+1} - 30u_k + 16u_{k-1} - u_{k-2}) = \frac{\partial^2 u}{\partial x_i^2} + \mathcal{O}(h_i^4), \\
D_{x_i,x_j} u = D_{x_i} D_{x_j} u &= \frac{\partial^2 u}{\partial x_i \partial x_j} + \mathcal{O}(h_i^4) + \mathcal{O}(h_j^4) + \mathcal{O}(h_i^4 h_j^4).
\end{aligned}$$

One disadvantage of these large stencils is that they are not easily applicable to points close to the boundary. In order to avoid the introduction of ghost points, we use standard second order stencils at the boundary. Since the coefficient functions $\alpha_{i,j}$, β_i vanish at all boundaries except at $x_1 = x_1^{\max}$, we do not expect a decrease in the accuracy of the scheme. In the time domain we use implicit Euler time stepping, which leads to a stable scheme and to order one in time. We use the transformation $t_f = T - t$ to step forward in time. In order to analyse the stability, we apply the classical von Neumann analysis, where the Fourier components are considered

$$u^k_{j_1,\dots,j_d}(x_1,\dots,x_d) = \xi^k \exp\Big(\mathrm{i}(\omega_1 x_1 + \cdots + \omega_d x_d)\Big),$$

where k is the time level, ξ denotes the amplitude, ω_i are the wave numbers and i is the imaginary unit. For simplicity we use fixed coefficients a_{jl}, b_j instead of the coefficient functions α_{jl} and β_j for $j,l = 1,\dots,d$ and equidistant step sizes $\Delta = h_1 = \cdots = h_d$. Let Δ_t denote the step size in time, then we can define the mesh ratio $\lambda = \frac{\Delta_t}{12\Delta^2}$. Substituting the Fourier components into our numerical scheme, we obtain

$$\begin{aligned}
&\left|\frac{\xi^{k+1}}{\xi^k}\right|^2 \\
&\quad = \Bigg(\Bigg[1 + r\Delta_t + 4\lambda\Big[\sum_{j=1}^d a_{jj}\Big(\frac{15}{2} - 8\cos(\omega_j\Delta) + \frac{1}{2}\cos(2\omega_j\Delta)\Big) \\
&\qquad +2\sum_{j=2}^d\sum_{l=1}^{j-1} a_{jl}\frac{1}{\sqrt{12}}(8\sin(\omega_j\Delta)-\sin(2\omega_j\Delta))\frac{1}{\sqrt{12}}(8\sin(\omega_l\Delta)-\sin(2\omega_l\Delta))\Big]\Bigg]^2 \\
&\qquad + \Bigg[\lambda\sum_{j=1}^d b_j\big(16\sin(\omega_j i\Delta) - 2\sin(2\omega_j\Delta)\big)\Bigg]^2\Bigg)^{-1}.
\end{aligned}$$

The amplification factor $\left|\frac{\xi^{k+1}}{\xi^k}\right|$ is smaller or equal to one if the denominator is equal or bigger than one. If we assume the worst case scenario where all b_i are equal to zero, this stability condition is satisfied if

$$\begin{aligned}
&\sum_{j=1}^d a_{jj}\Big(\frac{15}{2} - 8\cos(\omega_j\Delta) + \frac{1}{2}\cos(2\omega_j\Delta)\Big) \\
&+ 2\sum_{j=2}^d\sum_{l=1}^{j-1} a_{jl}\frac{1}{\sqrt{12}}\Big(8\sin(\omega_j\Delta) - \sin(2\omega_j\Delta)\Big)\frac{1}{\sqrt{12}}\Big(8\sin(\omega_l\Delta) - \sin(2\omega_l\Delta)\Big) \geq 0.
\end{aligned}$$

Defining $x_j = \frac{1}{\sqrt{12}}(8\sin(\omega_j\Delta) - \sin(2\omega_j\Delta))$ for $j = 1,\dots,d$, this is equivalent to

$$x^T A x + \sum_{j=1}^d a_{jj}\Big(\frac{-8}{3}(-5 + \cos(\omega_j\Delta))\sin\big(\frac{1}{2}\omega_j\Delta\big)^6\Big) \geq 0,$$

where $A = (a_{jl})$. Hence the scheme is stable if A is positive definite.

4. Combination technique and sparse grids

The discretisation of high dimensional PDEs on a tensor based grid leads to an exponentially growing number of grid nodes. This tremendous increase of the complexity either leads to an excessive memory consumption or to unreasonable run times. With the help of sparse grids the number of grid points can significantly be reduced. Let $h_n = 2^{-n}$ denote the mesh size at refinement level n on the d-dimension unit cube, then $\mathcal{O}(h_n^{-d})$ grid points belong to the full grid, whereas the sparse grid only consists of $\mathcal{O}(h_n^{-1}\log(h_n^{-1})^{d-1})$ nodes. The computation of the sparse grid solution can be performed with the so-called combination technique. It is based on combining a sequence of solutions with different step sizes in such a way that low order error terms cancel out. The combination technique reads

$$u_n^s = \sum_{q=0}^{d-1}(-1)^q\binom{d-1}{q}\sum_{|\mathbf{l}|_1=n+d-1-q} u_{\mathbf{l}}$$

with multi-index $\mathbf{l} = (l_1, \ldots, l_d)$ and step sizes $h = \left(2^{-l_1}, \ldots, 2^{-l_d}\right)$. The numerical sub-solutions $u_{\mathbf{l}}$ are computed on the discrete grid defined via the level $\mathbf{l}$. The sparse grid solution on refinement level n is denoted by u_n^s. In the following we switch our notation and denote the numerical sub-solution computed on the discrete grid Ω_h by u_h. If we assume that the error of each of the sub-solutions is of the form

$$u(\mathbf{x}) - u_h(\mathbf{x}) = \sum_{i=1}^{d}\sum_{\substack{\{j_1,\ldots,j_i\}\\ \subset\{1,\ldots,d\}}} h_{j_1}^4 \cdot \cdots \cdot h_{j_i}^4\,\omega_{j_1,\ldots,j_i}(\mathbf{x}; h_{j_1}, \ldots, h_{j_i}) \tag{3}$$

for $\mathbf{x} \in \Omega_h$, then we can expect for the combined solution a pointwise error of size

$$|u_n^s - u| \leq \mathcal{O}(h_n^4 \log(h_n^{-1})^{d-1}).$$

Bungartz et al. in [**1**] were the first ones, who proved with the help of Fourier series of discrete and semi-discrete solutions that such an error splitting structure holds for a second order finite difference solution[1] of the Laplace equation. Reisinger [**7**] recently showed that such a splitting also holds for a wider class of linear PDEs, e.g., convection-diffusion equations. He gives general conditions which need to be fulfilled to ensure the existence of the desired splitting structure: sufficiently smooth and compatible data, a consistent numerical scheme, which provides a truncation error of the desired mixed order, and a stable scheme. Unfortunately, this pointwise error only holds for the points, which belong to all sub-grids. The other discrete points are subject to the interpolation routine which is used to extent the discrete solution to combine them to the sparse grid solution. As there is only one inner point, the midpoint which belongs to all sub-grids, and because we are usually interested in a high order of convergence on the complete domain, e.g., in the maximum norm, this result seems to be rather limiting. In Figure 2 multi-linear interpolation has been used to combine the sub-solutions. While we see a high rate of convergence at the midpoint, there is only a low rate of convergence in the maximum norm. This example points out that linear interpolation cannot preserve the error structure and deteriorates the high order of our FDS.

Thus an interpolation technique is needed which can preserve the error splitting structure on the complete domain. We demand that the interpolation routine P

[1]leading to an error splitting of the same structure, but with order two

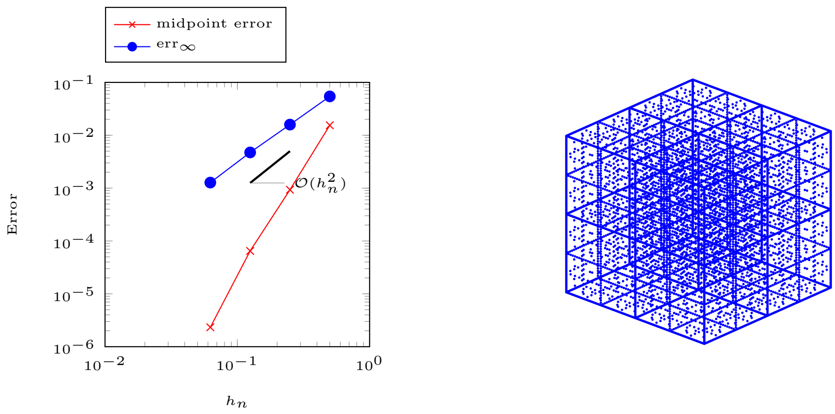

Figure 2. Pointwise error using multi-linear interpolation in the Combination Technique and 3d Sparse grid.

has a similar splitting structure to the finite difference solution (3)

$$
\begin{aligned}
&u(x_1,x_2) - (Pu_{h_1,h_2})(x_1,x_2) \\
&= \gamma_1(x_1,x_2;h_1)h_1^4 + \gamma_2(x_1,x_2;h_2)h_2^4 + \gamma_{1,2}(x_1,x_2;h_1,h_2)h_1^4h_2^4
\end{aligned} \tag{4}
$$

for all $(x_1,x_2) \in \Omega$ and bounded γ_1, γ_2, $\gamma_{1,2}$. Please note that we sketch the derivation of the splitting structure in two dimensions. The derivation for the higher dimensional case lies beyond the scope of this article, but basically follows by the same steps. In order to derive such a structure, we restrict ourselves to linear interpolation operators, and similar to [**7**], rewrite the error

$$
\begin{aligned}
&u(x_1,x_2) - (Pu_{h_1,h_2})(x_1,x_2) \\
&= u(x_1,x_2) - (Pu_{\Omega_h})(x_1,x_2) + (Pu_{\Omega_h})(x_1,x_2) - (Pu_{h_1,h_2})(x_1,x_2) \\
&= \underbrace{\underbrace{u(x_1,x_2) - (Pu_{\Omega_h})(x_1,x_2)}_{I} + \underbrace{(P(\underbrace{u_{\Omega_h} - u_{h_1,h_2}}_{II}))(x_1,x_2)}_{III}}_{IV},
\end{aligned}
$$

where u_{Ω_h} denotes the analytical solution on the discrete grid Ω_h. This enables us to analyse each error term separately. In the remainder of this section, we restrict ourselves to function spaces with sufficiently smooth mixed derivatives which are bounded by a constant C. The structure of the interpolation error (I) is given in [**3**], using univariate cubic spline interpolation in a tensor product approach:

$$
\begin{aligned}
&u(x_1,x_2) - (Pu_{\Omega_h})(x_1,x_2) \\
&= h_1^4c_1(x_1,x_2;h_1) + h_2^4c_2(x_1,x_2;h_2) + h_1^4h_2^4c_{1,2}(x_1,x_2;h_1,h_2),
\end{aligned}
$$

where the error terms are bounded by

$$\|c_1\|_\infty \le \frac{5}{384}C, \qquad \|c_2\|_\infty \le \frac{5}{384}C, \qquad \|c_{1,2}\|_\infty \le \frac{5^2}{384^2}C.$$

The pointwise error splitting (II) can be derived with the framework given in [**7**] and is based on the consistency of the numerical scheme. Therefore, we consider the given PDE (2) and its (spatial) discrete counterpart

$$\frac{\partial u}{\partial t} + Lu = 0, \qquad\qquad \frac{\partial u}{\partial t} + L_h u_h = g_h,$$

where g_h denotes the discretised boundary values. We emphasise that we intent to construct a space sparse grid and not a time-space sparse grid. We can express the truncation error via

$$(5) \qquad \big(L - L_h\big)u + g_h = h_1^4\tau_1(.;h_1) + h_2^4\tau_2(.;h_2) + h_1^4h_2^4\tau_{1,2}^{(0)}(.;h_1,h_2).$$

For simplicity we assume all coefficient functions to be bounded by one. Then we can compute bounds for the truncation errors

$$\|\tau_1\|_\infty \le \frac{1}{9}C, \qquad \|\tau_2\|_\infty \le \frac{1}{9}C, \qquad \|\tau_{1,2}^{(0)}\|_\infty \le \frac{1}{450}C.$$

We define the two auxiliary problems to describe the truncation errors τ_1, τ_2 in (5)

$$L_h^{(1)}\omega_1(.;h_1) = \tau_1(.;h_1), \qquad\qquad L_h^{(2)}\omega_2(.;h_2) = \tau_2(.;h_2),$$

where the operators $L_h^{(i)}$ for $i = 1, 2$, are semi-discretisations of L, denoting the discretisation in coordinate direction i only. If the numerical scheme and also its semi-discretisations are stable, one can receive bounds for the solutions

$$\|\omega_i\| = \|L_h^{(i)^{-1}}\tau_i\| \le \|L_h^{(i)^{-1}}\|\|\tau_i\| \le \|\tau_i\| \qquad \text{for } i = 1, 2.$$

Please note that this also holds for derivatives of ω_i, τ_i, respectively, which can be seen by differentiation of the auxiliary problems. By subtraction of the solutions of the semi-discrete problems from the truncation error, we obtain

$$\begin{aligned}&\big(L - L_h\big)u + g_h - h_1^4L_h\omega_1(.;h_1) - h_2^4L_h\omega_2(.;h_2)\\ &= h_1^4\big(L_h^{(1)} - L_h\big)\omega_1(.;h_1) + h_2^4\big(L_h^{(2)} - L_h\big)\omega_2(.;h_2) + h_1^4h_2^4\tau_{1,2}^{(0)}(.;h_1,h_2).\end{aligned}$$

Further, we get by expansion

$$\begin{aligned}\big(L_h^{(1)} - L_h\big)\omega_1(.;h_1) &= h_2^4\nu_{1;2}(.;h_1,h_2) + h_1^4h_2^4\nu_{1;1,2}(.;h_1,h_2)\\ \big(L_h^{(2)} - L_h\big)\omega_2(.;h_2) &= h_1^4\nu_{2;1}(.;h_1,h_2) + h_1^4h_2^4\nu_{2;1,2}(.;h_1,h_2),\end{aligned}$$

where $\|\nu_{1;2}\|_\infty \le \frac{1}{9^2}C$, $\|\nu_{2;1}\|_\infty \le \frac{1}{9^2}C$, $\|\nu_{1;1,2}\|_\infty \le \frac{1}{450^2}C$ and $\|\nu_{2;1,2}\|_\infty \le \frac{1}{450^2}C$. The bounds can easily be verified by straightforward Taylor expansion and the argumentation given above. Hence we get

$$\begin{aligned}&\big(L-L_h\big)u+g_h-h_1^4L_h\omega_1(.;h_1)-h_2^4L_h\omega_2(.;h_2)\\&=\ h_1^4h_2^4\big(\tau_{1,2}^{(0)}(.;h_1,h_2)+\nu_{1;2}(.;h_1,h_2)+\nu_{2;1}(.;h_1,h_2)\\&\quad+h_1^4\nu_{1;1,2}(.;h_1,h_2)+h_2^4\nu_{2;1,2}(.;h_1,h_2)\big)\\&=:\ h_1^4h_2^4\tau_{1,2}^{(1)}(.;h_1,h_2)\end{aligned}$$

with bounds $\|\tau_{1,2}^{(1)}\|_\infty\le\big(\frac{1}{450}+2\frac{1}{9^2}+2\frac{1}{450^2}\big)\,C$. Applying L_h^{-1} from the left gives

$$u-u_h=h_1^4\omega_1(.;h_1)+h_2^4\omega_2(.;h_2)+h_1^4h_2^4\underbrace{L_h^{-1}\tau_{1,2}^{(1)}(.;h_1,h_2)}_{=:\omega_{1,2}(.;h_1,h_2)}.$$

The stability of the numerical scheme leads to $\|\omega_{1,2}\|_\infty\le\big(\frac{1}{450}+2\frac{1}{9^2}+2\frac{1}{450^2}\big)\,C$. In a next step this error can be interpolated to derive the term (III). Exploiting the linearity of the interpolation operator P and the fact that the derivatives of ω_1, ω_2, $\omega_{1,2}$ are bounded, we conclude

$$\big(P(u_{\Omega_h}-u_{h_1,h_2})\big)(.)=h_1^4\zeta_1(.;h_1)+h_2^4\zeta_2(.;h_2)+h_1^4h_2^4\zeta_{1,2}(.;h_1,h_2)$$

with bounded coefficient functions

$$\|\zeta_1\|_\infty\le\left(\frac{1}{9}+\frac{1}{9}\frac{5}{384}\right)C,\quad \|\zeta_2\|_\infty\le\left(\frac{1}{9}+\frac{1}{9}\frac{5}{384}\right)C,\quad \|\zeta_{1,2}\|_\infty\le\frac{228131773}{7464960000}C.$$

The combination of (I) and (III) yields the desired splitting structure (4) with bounded coefficient functions

$$\|\gamma_1\|_\infty\le\frac{217}{1728}C,\quad \|\gamma_2\|_\infty\le\frac{217}{1728}C,\quad \|\gamma_{1,2}\|_\infty\le\frac{114698699}{3732480000}C.$$

5. Numerical example

In this section, we want to test our theoretical findings and considerations by a practical example. Therefore, we compute the value of an European plain vanilla put basket option of an equally weighted basket with the following option and market parameters: the time to maturity is $T=1$, the strike price is $K=40$ and the risk free interest rate is set to $r=0.06$. The domain in the first coordinate direction is truncated at $x_1^{\max}=3K$ and implicit time stepping with step size $\Delta_t=0.01$ is used. The dividend is chosen to be $q_i=0$ for $i=1,\dots,d$. The volatility for all assets is set to $\sigma_i=0.3$ for $i=1,\dots,d$ and the correlation is given by

$$\rho=\begin{pmatrix}1&0.3&0.4&0.5\\0.3&1&0.2&0.25\\0.4&0.2&1&0.3\\0.5&0.25&0.3&1\end{pmatrix}.$$

As we want to evaluate if the high order of convergence can be seen in practice on the whole domain, we compute the error in the discrete maximum norm on the last time layer $t_f=T$.

$$e_\infty^n:=\|u_n^s-R_sU\|_\infty,$$

where the operator R_s restricts the solution vector of a highly accurate numerical solution U to the sparse grid. Table 1 shows the accuracy of our sparse grid solution in up to four dimensions. In the two and three dimensional cases we see a high rate of convergence as we would have expected from the theoretical results. However we do not have a high convergence in the four dimensional case. This might be due to the fact that we have not reached the asymptotic region and a further refinement is needed. In Figure 3, we compare the number of grid points to the

n	2d		3d		4d	
	e_∞^n	$e_\infty^{n-1}/e_\infty^n$	e_∞^n	$e_\infty^{n-1}/e_\infty^n$	e_∞^n	$e_\infty^{n-1}/e_\infty^n$
2	9.3764e-1					
3	1.5926e-1	5.89				
4	1.9547e-2	8.15	1.02892			
5	1.5353e-3	12.73	1.61872e-1	6.36	1.0552	
6	1.3272e-4	11.57	2.41938e-2	6.69	1.6485e-1	6.40
7	1.0072e-5	13.18	2.16649e-3	11.17	2.3023e-2	7.16

Table 1. Accuracy results.

reached accuracy. If the number of grid points is taken as an indicator of memory usage and of runtime, the high order sparse grid approach clearly outperforms the full grid approach. The combined solution is roughly about ten times more accurate if the same number of nodes is employed.

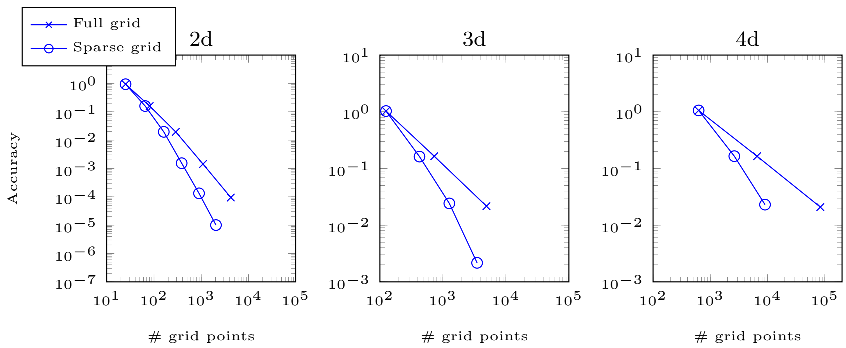

Figure 3. Number of grid points versus accuracy.

6. Conclusion and outlook

In this paper, we have presented a high order sparse grid solution for European plain vanilla basket options. The deterioration coming from the non-differentiability at the strike price could be remedied via a coordinate transformation and smoothing of the initial data. It has been shown that the extension of the discrete subsolutions with a tensor product based cubic spline interpolation approach can preserve the high accuracy and splitting structure. Based on the theoretical findings, we tested our schemes numerically and validated our results.

In a future, we will apply more sophisticated schemes to compute the subsolutions. High order compact schemes seem to be the first choice since they circumvent large stencils and provide highly accurate solutions.

References

1. Bungartz H.-J., Griebel M., Röschke D. and Zenger C., *Pointwise Convergence Of The Combination Technique For Laplace's Equation*, East-West J. Numer. Math **2** (1994), 21–45.

2. Griebel M., Schneider M. and Zenger C., *A Combination Technique for the Solution of Sparse Grid Problems*, IMACS Elsevier, Iterative Methods in Linear Algebra (1992), 263–281.

3. Hendricks C., Ehrhardt M. and Günther M., *High order tensor product interpolation in the Combination Technique*, preprint, 14/25 University of Wuppertal 2014.

4. Kreiss H. O., Thomée V. and Widlund O., *Smoothing of initial data and rates of convergence for parabolic difference equations*, Communications on Pure and Applied Mathematics **23(2)** (1970), 241–259.

5. Leentvaar C. and Oosterlee C., *On coordinate transformation and grid stretching for sparse grid pricing of basket options.* J. Comput. Appl. Math. (Special Issue: Numerical Methods in Finance) **222(1)** (2008), 193–209.

6. Reisinger C., *Numerische Methoden für hochdimensionale parabolische Gleichungen am Beispiel von Optionspreisaufgaben*, PhD thesis, Ruprecht-Karls-Universität Heidelberg, 2004.

7. Reisinger C., *Analysis of Linear Difference Schemes in Sparse Grid Combination Technique*, IMA J. Numer. Anal. **33(2)** (2013), 544–581.

8. Zenger C., *Sparse grids for the Schrödinger equation*, In Parallel Algorithms for Partial Differential Equations, volume 72. Vieweg, 1991.

C. Hendricks, M. Ehrhardt and M. Günther, Gaußstr. 20, 42119 Wuppertal, Germany, *e-mail*: {hendricks,ehrhardt,guenther}@math.uni-wuppertal.de